

## Electrochemical Voltage Spectroscopy for Analysis of Nickel Electrodes

10 January 2000

Prepared by

L. H. THALLER, A. H. ZIMMERMAN, and G. A. TO  
Electronics Technology Center  
Technology Operations

Prepared for

SPACE AND MISSILE SYSTEMS CENTER  
AIR FORCE MATERIEL COMMAND  
2430 E. El Segundo Boulevard  
Los Angeles Air Force Base, CA 90245

20000223 116

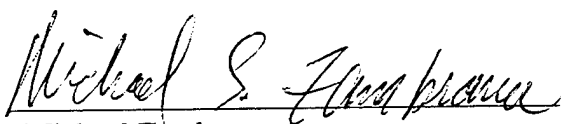
Engineering and Technology Group

APPROVED FOR PUBLIC RELEASE;  
DISTRIBUTION UNLIMITED

This report was submitted by The Aerospace Corporation, El Segundo, CA 90245-4691, under Contract No. F04701-93-C-0094 with the Space and Missile Systems Center, 2430 E. El Segundo Blvd., Los Angeles Air Force Base, CA 90245. It was reviewed and approved for The Aerospace Corporation by B. Jaduszliwer, Principal Director, Electronics Technology Center. Michael Zambrana was the project officer for the Mission-Oriented Investigation and Experimentation (MOIE) program.

This report has been reviewed by the Public Affairs Office (PAS) and is releasable to the National Technical Information Service (NTIS). At NTIS, it will be available to the general public, including foreign nationals.

This technical report has been reviewed and is approved for publication. Publication of this report does not constitute Air Force approval of the report's findings or conclusions. It is published only for the exchange and stimulation of ideas.

A handwritten signature in dark ink, reading "Michael S. Zambrana". The signature is fluid and cursive, with the first name "Michael" being the most prominent part.

Michael Zambrana  
SMC/AXE

REPORT DOCUMENTATION PAGE			Form Approved OMB No. 0704-0188	
Public reporting burden for this collection of information is estimated to average 1 hour per response, including the time for reviewing instructions, searching existing data sources, gathering and maintaining the data needed, and completing and reviewing the collection of information. Send comments regarding this burden estimate or any other aspect of this collection of information, including suggestions for reducing this burden to Washington Headquarters Services, Directorate for Information Operations and Reports, 1215 Jefferson Davis Highway, Suite 1204, Arlington, VA 22202-4302, and to the Office of Management and Budget, Paperwork Reduction Project (0704-0188), Washington, DC 20503.				
1. AGENCY USE ONLY (Leave blank)		2. REPORT DATE 19 January 2000		3. REPORT TYPE AND DATES COVERED
4. TITLE AND SUBTITLE  Electrochemical Voltage Spectroscopy for analysis of Nickel Electrodes			5. FUNDING NUMBERS  F04701-93-C-0094	
6. AUTHOR(S)  L. H. Thaller, A. H. Zimmerman, and G. A. To				
7. PERFORMING ORGANIZATION NAME(S) AND ADDRESS(ES) The Aerospace Corporation Technology Operations El Segundo, CA 90245-4691			8. PERFORMING ORGANIZATION REPORT NUMBER  TR-2000(8555)-3	
9. SPONSORING/MONITORING AGENCY NAME(S) AND ADDRESS(ES) Space and Missile Systems Center Air Force Materiel Command 2430 E. El Segundo Boulevard Los Angeles Air Force Base, CA 90245			10. SPONSORING/MONITORING AGENCY REPORT NUMBER  SMC-TR-00-02	
11. SUPPLEMENTARY NOTES				
12a. DISTRIBUTION/AVAILABILITY STATEMENT  Approved for public release; distribution unlimited			12b. DISTRIBUTION CODE	
13. ABSTRACT (Maximum 200 words)  Electrochemical Voltage Spectroscopy (EVS) is a technique that directly measures the density of electrochemically active states in an electrode as a function of the applied voltage. In EVS measurements, the voltage of an electrode is scanned at a rate that is slow enough to maintain the electrode close to thermodynamic equilibrium, over a potential range where electroactive species may be oxidized or reduced. The density of reactive sites is obtained from the coulombs of charge passed through the electrode per voltage increment, which is essentially differential capacitance. For most electrodes, interest is primarily in the Faradaic components of the EVS spectra, which exhibit sharp peaks at the electrochemical redox potentials, although non-Faradaic components (such as double-layer or surface capacitance) can also be measured. For nickel electrodes, EVS provides an extremely useful method for probing the phase composition of the active material based on subtle differences in redox potentials. Alternatively, EVS can detect trace levels of electroactive contaminants in nickel-hydrogen cells or nickel electrodes by scanning the potential over the redox range for the contaminant of interest. We will discuss the use of nickel electrode EVS signatures to indicate cobalt additive levels, sinter corrosion, surface changes, double-layer capacitance, electrode swelling, and other factors influencing the performance of the nickel electrode.				
14. SUBJECT TERMS  Nickel electrodes, Electrochemical voltage spectroscopy, redox potential			15. NUMBER OF PAGES 19	
			16. PRICE CODE	
17. SECURITY CLASSIFICATION OF REPORT UNCLASSIFIED	18. SECURITY CLASSIFICATION OF THIS PAGE UNCLASSIFIED	19. SECURITY CLASSIFICATION OF ABSTRACT UNCLASSIFIED	20. LIMITATION OF ABSTRACT	

## Contents

1. Background .....	1
2. Test Equipment .....	5
3. Test Electrodes .....	7
4. Test Results .....	9
4.1 Electrodes From a Good Cell .....	9
4.2 Differences Between Cycles One and Two .....	10
4.3 Electrode From a Cell Containing Nickel Oxide Hydroxide .....	10
4.4 Electrode From a Cell Suspected of Having Hydrogen Sickness .....	11
4.5 Study of a Electrode Sample Cycled to Different End-of-Charge Voltages .....	12
4.6 Sequential Cycling of the Same Sample of Electrode .....	13
4.7 Electrode Exposed to High-Pressure Hydrogen Gas .....	14
5. Summary .....	17
References .....	19

## Figures

1. EVS spectra for a nickel electrode from a NiCd cell .....	1
2. EVS spectra for a normally performing baseline nickel electrode .....	9
3. First EVS scan (dark line) compared to second EVS (light line) .....	10
4. EVS spectra of nickel electrode containing nickel oxide hydroxide .....	10
5. EVS spectra of a nickel electrode modified by reaction with hydrogen .....	11
6. EVS for a nickel electrode. Maximum scan voltage is 0.495 V. ....	12
7. EVS for nickel electrode. Maximum scan voltage is 0.500 V .....	12

8. EVS spectra after initial recharger to 0.5 V (light line), and after repeated partial recharges building up to 0.5 V (dark line).....	13
9. Loss of hydrogen pressure during open-circuit stand (from Ref. 5). ....	14
10. Cell configuration and test apparatus for hydrogen soak tests. ....	15
11. EVS spectra before exposure of charged nickel electrode to hydrogen gas. ....	15
12. EVS spectra before exposure of charged nickel electrode to hydrogen gas. ....	16

## Tables

I. Charge Efficiencies of Good Electrodes Charged To Different End-of-Charge Voltages.....	13
---	----

## 1. Background

Electrochemical Voltage Spectroscopy (EVS) is a subset of a class of electroanalytical techniques referred to as cyclic voltammetry. Cyclic voltammetry applies a linearly changing voltage to an electrode. The operator sets the rate of change of the sweep voltage as well as the span across which the voltage is scanned. A fuller description of this technique can be found in any basic treatment of electroanalytical methods.<sup>1</sup> EVS is differentiated from standard cyclic voltammetry by the very low rate at which the voltage is typically scanned, the variations in voltage scan rate frequently made during the test, and by the fact that the density of states is plotted as a function of applied voltage.

In either cyclic voltammetry or EVS the voltage span is frequently selected so that just one electrode reaction is observed. This approach is utilized in EVS studies of nickel electrodes, where the range of 0.2 to 0.52 V (vs. Hg/HgO) encompasses the normal charge and discharge reactions. Figure 1 provides an example of EVS data collected from a nickel electrode from an aerospace-type nickel-cadmium cell. In Figure 1, a negative charge density indicates electrode charging, and a positive charge density indicates discharge. The charge and discharge reactions in the nickel electrode are generally represented by reactions [1]–[3], with a non-electrochemical recrystallization process also acting to convert  $\alpha$ -Ni(OH)<sub>2</sub> back into  $\beta$ -Ni(OH)<sub>2</sub>.

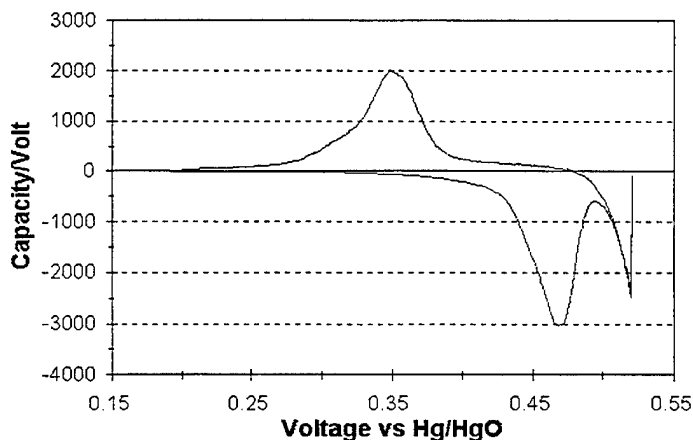
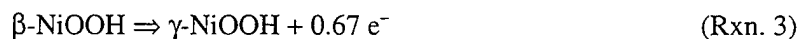
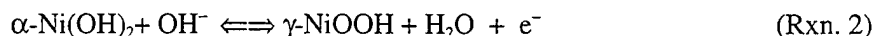
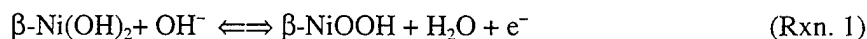
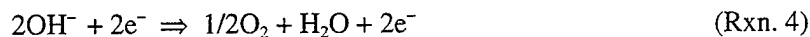


Figure 1. EVS spectra for a nickel electrode from a NiCd cell.

The redox potential of reaction 1 is about 40 mV higher than that of reaction [2], and the potential of both of these reactions tend to be decreased by increasing levels of cobalt additive. The kinetics of reaction [3] are quite slow, and significant overcharge is typically required to convert significant amounts of  $\beta$ -NiOOH to  $\gamma$ -NiOOH.

Because the nickel electrode in Figure 1 is from a NiCd cell, the small amounts of cadmium that it contains inhibit the formation of  $\gamma$ -NiOOH, thus providing a relatively simple EVS spectra dominated by the charge and discharge of the beta phases. An additional process, oxygen evolution (reaction [4]), is seen in the EVS spectra above 0.47–0.48 V (vs.Hg/HgO).



The distance between the zero point on the y-axis and the curve is a measure of the charge that is flowing into the electrode. The bell-like shape of the curve results from the gradual increase in the charging current as more and more driving force is applied to the reaction. After reaching the maximum point on the curve, the charging current becomes less, even though the driving force continues to increase. This occurs because as more and more of a fixed amount of chargeable material is converted to the charged form, the residual amount that remains uncharged approaches zero. The upswing in charge seen in Figure 1 at the highest voltages results from increasing oxygen evolution. Since there is a relatively unlimited amount of water in a flooded electrode situation, the amount of charge that can be consumed in this reaction is very large. The EVS scan is generally set to limit the voltage at a point where oxygen evolution is not excessive. At this point, the voltage scans in the opposite direction. In the case of a nickel electrode that is charged only to the beta phase, as in Figure 1, reaction [1] describes the discharge process.

Cyclic voltammetry is often used to evaluate the reversibility of the electrode reaction under study. The position of the peaks as recorded in a cyclic voltammetry study is indicative of the relative reversibility of the electrochemical reaction under study. The sweep rates used in typical voltammetry studies are much faster, and the voltage spans are much narrower than those used in EVS studies. Thus, EVS is not typically used to evaluate kinetic reversibility, but is well suited for study of reversible potentials, voltage hysteresis, and reaction rates as a function of potential and composition.

As the name implies, EVS is often used to detect the presence of small amounts of electrochemically active species that are present in the material under investigation. A more complete description of this technique is found elsewhere.<sup>2</sup> As used in our laboratory, EVS involves a computer that is programmed to control an ultra-slow sweep multichannel voltammetry instrument. Expanding the range of a test as shown in Figure 1 and using a sweep rate of only 2  $\mu\text{V/s}$  can be used to detect small quantities of electroactive impurities that might be impacting the performance of the cadmium electrode. The presence of nickel, iron, copper, and cobalt can be detected in nickel electrodes. Unlike the large, well-formed peaks displayed by the beta form of nickel active material Figure 1, low-level impurities will exhibit much smaller peaks. Tables of standard half-cell reactions may be used to identify these. The study to be reported here will address the use of EVS as an electroanalytical technique, where it has been found to be quite useful in detecting signatures of typical problems that occur in rechargeable nickel electrodes.

The EVS technique has been utilized to develop a database of signatures for numerous electrodes of varying structural, chemical, or degradation features. In many situations EVS signatures provide a significantly simpler and faster method for establishing the root causes for performance issues. This study also has provided baseline information for electrodes that were known to be free from any performance issue.



## 2. Test Equipment

The test equipment consisted of a PC containing the software to set up, monitor, and control up to 8 independent EVS experiments. This software operates on a Windows NT workstation, and enables registered users to control and monitor the tests from computers in their offices or other remote sites. The data from any test can be readily downloaded to a remote computer for processing or analysis. This equipment allowed the EVS scan rate to be adjusted as desired at any time during either a single scan or a given EVS test. For all the tests reported here, a constant scan rate of  $2\text{ }\mu\text{V/s}$  was used. The applied voltage was scanned in fixed steps of  $0.989\text{ mV}$  with 18-bit precision. At each applied voltage step, the equipment recorded the number of coulombs that were either charged into or discharged from the electrode. At the completion of the test, a charge density graph of the complete sweep was available as well as the data file used to prepare the charge density graph.

### 3. Test Electrodes

Samples were either cut from nickel electrodes that were taken from nickel-hydrogen cells that had completed varying amounts of life-cycle testing, or were made in our laboratory using standard electrochemical impregnation methods. Electrodes of either 30 or 35 mil thickness that measured 1.0 cm by 1.0 cm were welded inside a nickel mesh, which in turn was welded to a nickel lead wire. The counter electrode was a sheet of pure nickel foil. The reference electrode was a mercury/mercuric oxide electrode (Hg/HgO). The test electrode was placed in a flooded cell containing about 200 ml of 31.54% potassium hydroxide (KOH) solution. The cell was sealed against any intrusion of air. During these experiments, up to six tests were run at any one time. The sweep rate and voltage span were programmed into the computer and first involved an initial discharge of any residual charge that might be present in the electrode by sweeping at the rate of  $2 \mu\text{V/s}$  from the rest potential down to 0.2 V vs. Hg/HgO. The electrode was then charged to a preselected end-of-charge (EOC) voltage that was varied depending on the objective of the test, after which the voltage was scanned back down to 0.2 at the  $2 \mu\text{V/s}$  rate.

The following sections describe the different types of tests that were carried out as part of this study. Many samples of electrodes that were tested were also characterized extensively as part of post-test analyses carried out on cells that had undergone long-term life cycle testing. Electrodes that had suffered corrosion damage, severe swelling, performance degradation due to hydrogen sickness, and a newly discovered capacity loss related to the presence of nickel oxide hydroxide<sup>3</sup> were tested. Electrode material from a cell that had no performance problems and very few charge/discharge cycles was also tested to provide a performance baseline. Two studies unrelated to performance problems are also reported because they shed light on the general topic of nickel electrode performance in nickel-hydrogen cells.

## 4. Test Results

### 4.1 Electrodes From a Good Cell

Figure 2 shows a typical EVS spectra for an electrode that did not have any performance or degradation problems. This data is considered to be baseline data for this study. After being discharged to 0.2 V, it was scanned to an EOC voltage of 0.52 V. At about 0.45 V, the active material is first charged to the beta form of nickel oxyhydroxide where the average nickel valence is about 3.0. The peak just above 0.50 V is the charging of the beta-phase material to the gamma phase where the average valence is 3.67. As the rate of gamma-phase formation decreases, the onset of oxygen evolution is seen. Oxygen evolution is not absent at lower potentials, but in this example, it becomes the dominant reaction only after the gamma reaction subsides. At the point where the voltage has been scanned up to 0.52 V, the scan direction is reversed, and the peak appearing at about 0.27 V is the discharge of the gamma-phase material. Had there been any beta-phase material, it would have discharged at about 0.35 V. The charging portion of the cycle that went to a cutoff voltage of 0.52 V was high enough to convert all of the active material to the gamma phase for this electrode sample. The capacity of this 1-cm<sup>2</sup>, 35-mil-thick electrode, when charged to 0.52 V, was 52 mAh. The capacity is obtained by integrating the positive area under the trace during the voltage scan from about 0.43 V down to 0.2 V. When considering an entire electrode from a 3.5-in.-dia cell (about 50 cm<sup>2</sup>), this capacity corresponds to about 2.6 AH. This capacity corresponds to about 152% utilization, and is much higher than the useable capacity of an electrode in the starved condition inside an actual cell, which is typically limited to 100–110% utilization.

Figure 3 was obtained by cycling a sample of the same electrode that was shown in Figure 2. The difference here was that the first and second cycles are shown on the same figure. It should be noted that the beginning of the beta material recharge is delayed during the first cycle compared to the one that immediately follows it. The beta peak for the first cycle occurs at about 0.49 V, whereas the same peak appears at about 0.45 V during the second cycle. As with the sample depicted in Figure 1,

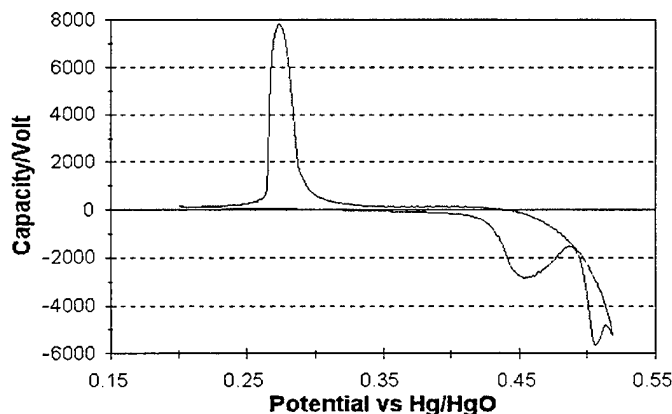


Figure 2. EVS spectra for a normally performing baseline nickel electrode.

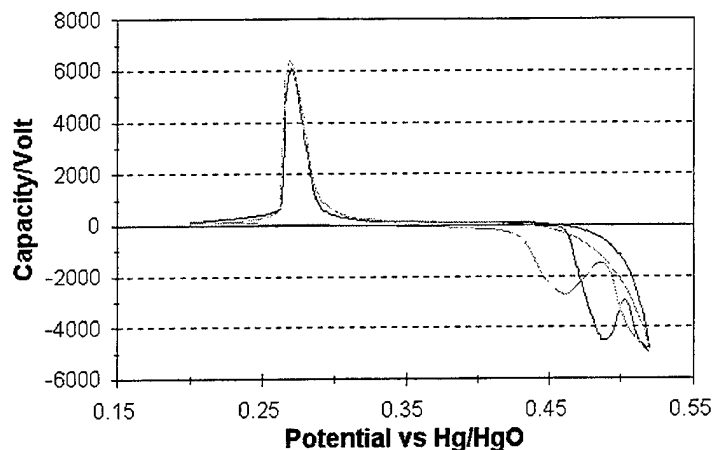


Figure 3. First EVS scan (dark line) compared to second EVS (light line).

#### 4.2 Differences Between Cycles One and Two

the EOC was selected to be 0.52 V. The discharge peaks are located at the same position and have essentially the same capacity as judged by the area under the curves. This behavior is reminiscent of what is called a "wakeup" cycle in nickel-cadmium and nickel-hydrogen cells. Apparently, there are multiple states in which the discharged form of nickel hydroxide can reside if it is allowed to remain in the discharged state for extended periods of time. This type of phenomenon was detected in NiCd and NiH<sub>2</sub> cells by Zimmerman<sup>4</sup> during thermal measurement studies, and was also evidenced by differences in the charging curves. This phenomenon was attributed to Ostwald ripening that occurs in the discharged form of nickel hydroxide present in nickel electrodes.

#### 4.3 Electrode From a Cell Containing Nickel Oxide Hydroxide

Figure 4 was obtained from EVS tests on a nickel electrode from a cell in which there was a large amount of an unusual material known as nickel oxide hydroxide (Ni<sub>2</sub>O<sub>3</sub>H). This material can be

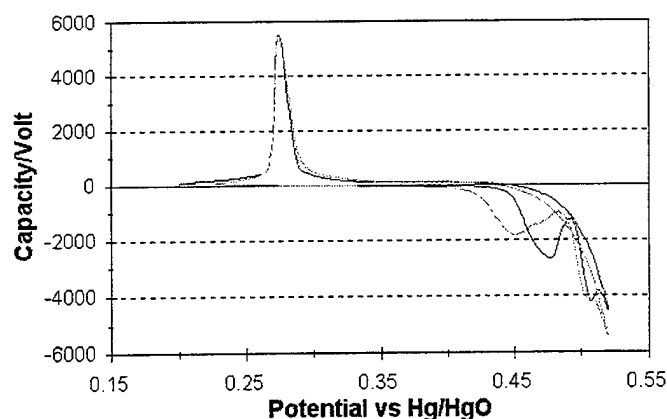


Figure 4. EVS spectra of nickel electrode containing nickel oxide hydroxide. Dark line is scan 1, and lighter line is scan 2.

formed in cells that are significantly overcharged, resulting in large amounts of heat and highly oxidizing conditions. In this material, the average valence of nickel is 2.5. This material is completely electrochemically inactive. Its presence is detected by subjecting a fully discharged sample of the active material to an analysis for charged material. This material can also be identified by its X-ray diffraction pattern<sup>3</sup> and by its thermogravimetric signature. Figure 4 shows a typical positioning of the charge and discharge peaks, but the area under the discharge peak indicates that there is a lower than normal amount of capacity in the sample of the electrode that underwent the test. The integrated area for this sample measured only 32.1 and 28.8 mAh for the two electrodes on which this test was carried out. In the test described in Subsection B for a normal nickel electrode, about 50 mAh were available during the discharge portion of the sweep. The cell from which this sample of nickel electrode came displayed a severe loss of capacity during its life cycle test. This signature is different from an electrode that has suffered loss of capacity and reduced charge efficiency due to what is known as "hydrogen sickness."

#### 4.4 Electrode From a Cell Suspected of Having Hydrogen Sickness

Figure 5 is an example of the signature of electrode material that has experienced a reduction in the usable capacity and in the charge efficiency like the previous example. However the signature is quite different. In this example, a distinct beta peak is seen following the charging scan up to a 0.52-V cutoff. As noted in earlier examples, charging to this high voltage should have resulted in an absence of any beta material during the subsequent discharge. Hydrogen sickness results from the irreversible partial depletion of cobalt from the lattice sites of the nickel hydroxide material that is immediately adjacent to the surface of the nickel metal current collector. This results in non-cobalt containing regions of active material, which have an elevated electrochemical potential, at the current collector surface. Since cobalt-depleted active material has about a 30–40 mV higher redox potential, it is much more difficult to charge it to the gamma form of the active material when charging to the same EOC voltage. Potentials where the formation of gamma-phase material occurred at a significant rate now are dominated by the evolution of oxygen gas.

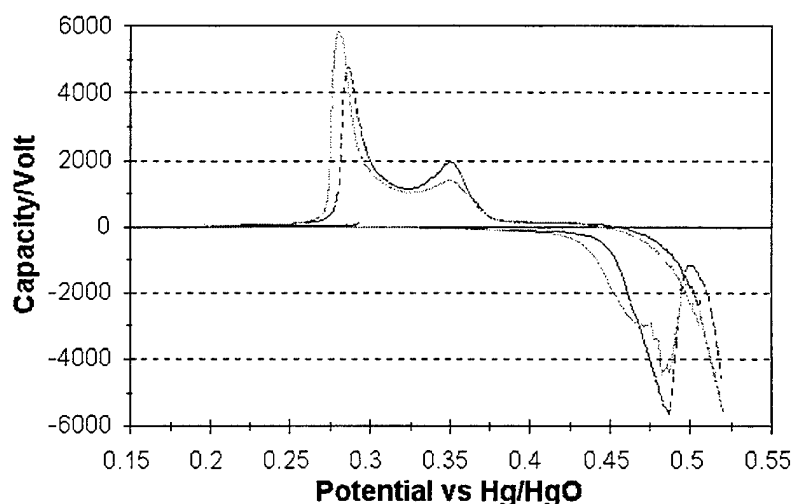


Figure 5. EVS spectra of a nickel electrode modified by reaction with hydrogen. The dark line is scan 1, and the light line is scan 2.

#### 4.5 Study of a Electrode Sample Cycled to Different End-of-Charge Voltages

Figure 6 and 7 were obtained during a test carried out on a sample of good electrode material that was cycled to different EOC voltages. In this test, a different sample of material was used for each test. Each electrode was cycled twice, with only the second sweep being shown here. In comparing the scans in Figures 6 and 7, the significant difference that results from only a 5-mV difference in EOC voltage should be noted. The sample in Figure 6 was charged to 0.495 V, whereas the sample in Figure 7 was charged to 0.50 V. As would be expected, charging to higher and higher EOC voltages resulted in larger amounts of usable capacity when the beta and the gamma peaks were summed together. As the EOC voltages went to progressively higher values, the charge efficiency was decreased since larger amounts of the charge current went to form oxygen in parallel with the formation of the higher-capacity gamma material. The ratio of the discharge capacity to the charge capacity is a measure of the charge efficiency of this sample piece of electrode. This number varies as the EOC voltage is varied. Table I is a summary of the results of this set of experiments, showing that as the EOC voltage is increased, there is an increase in the capacity during the discharge portion of the sweep as well as a reduction in the charge efficiency. By charging to higher EOC voltages, more of the beta form of the charged material is converted to the higher-capacity gamma phase. At the same time, however, a larger percentage of the charging current is consumed by the evolution of oxygen.

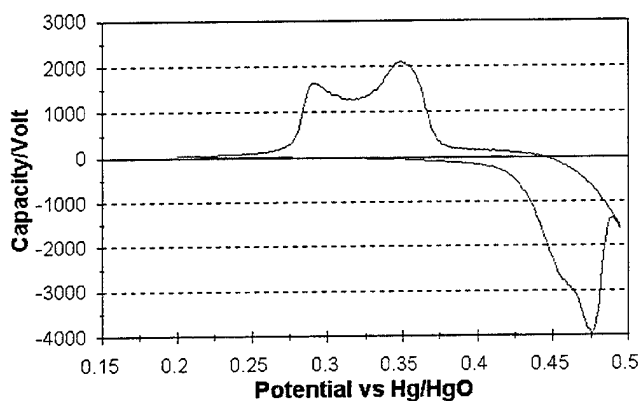


Figure 6. EVS for a nickel electrode. Maximum scan voltage is 0.495 V.

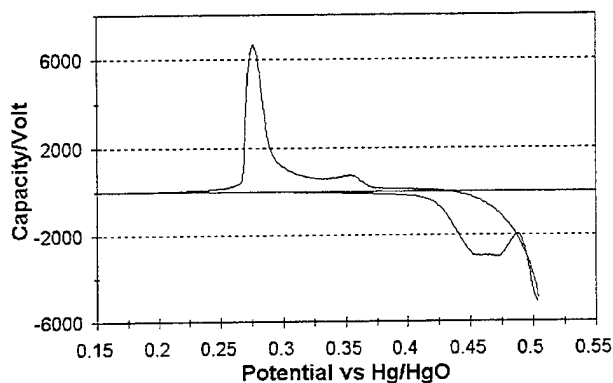


Figure 7. EVS for nickel electrode. Maximum scan voltage is 0.500 V.

Table I. Charge Efficiencies of Good Electrodes  
Charged To Different End-of-Charge Voltages

EOC Voltage vs. Hg/HgO	mAh In	mAh Out	Charge Eff-%
0.540	223.2	55.9	25.1
0.520	142.4	54.4	38.2
0.510	108.4	52.5	48.4
0.505	87.1	51.7	59.4
0.500	72.3	45.7	63.2
0.495	55.7	44.5	79.9
0.490	44.5	40.8	85.9
0.485	40.8	36.9	92.0
0.480	36.9	32.2	96.7
0.470	22.1	21.7	98.3

#### 4.6 Sequential Cycling of the Same Sample of Electrode

Figure 8 contains several unique signatures. The electrode sampled in this test was produced in our laboratory and appears to display a doublet in the charging of the beta material rather than a distinct beta and gamma peak prior to the onset of full oxygen evolution. The electrode was made by impregnating slurry plaque material using an aqueous process. The electrode depicted in Figure 8 had a 5% level of cobalt doping. After 500 charge/discharge cycles to stabilize performance, the discharge peak on the left in Figure 8 was obtained by scanning up to 0.50 V, which consists primarily of gamma-phase material. The discharge curve on the right was obtained in separate experiments where the same electrode was charged first to 0.52 V, followed by a series of cycles ending first at 0.46 V and progressing up 5 mV at a time each cycle thereafter. The curve shown in Figure 8 (dark line) is the curve for the final cycle, which scanned up to the 0.50-V EOC level, and exhibited essentially beta-phase material only. It is interesting that the same cyclic voltage span that initially charged the electrode fully to the gamma phase gave essentially no gamma phase after a few partial

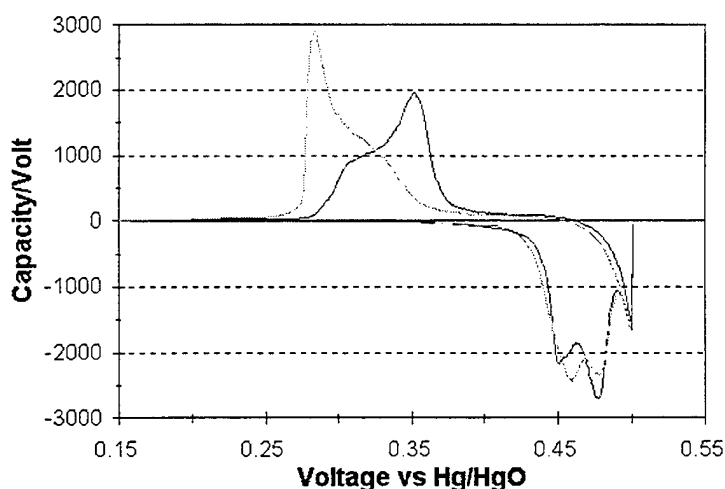


Figure 8. EVS spectra after initial recharger to 0.5 V (light line), and after repeated partial recharges building up to 0.5 V (dark line).

recharge cycles. It would appear that cycling from a fully discharged state to a partially charged state results in some unusual phase distributions or layers in the active material, resulting in at least a temporary reduction in the chargeability of the active material.

#### 4.7 Electrode Exposed to High-Pressure Hydrogen Gas

A series of tests were conducted to determine how hydrogen gas exposure affects the phases in the charged nickel electrode. The electrodes used in these tests were new samples of electrodes taken from a cell that had seen very little cycling and had shown no sign of any degradation problems. The object of the experiments was to investigate the sequential mechanisms involved in the self-discharge reactions of the nickel electrode. Studies by Ritterman,<sup>5</sup> Suresh,<sup>6</sup> and more recently by Pralong<sup>7</sup> have noted what appeared to be two different rates at which the pressure decreased during the open-circuit stand periods of nickel-hydrogen cells. Figure 9 is from the study by Ritterman, where the two distinct regions are clearly seen. In the paper by Pralong, it was suggested that the initial rapid rate of pressure loss was due to the self-discharge of the gamma phase of the charged active material while the lower rate of pressure loss was due to the self-discharge of the beta material. Since EVS techniques very easily distinguish the difference between the amount of gamma phase and the beta phase, an experiment was configured to explore this issue. The preliminary results have been encouraging in terms of being able to distinguish between the relative amounts of beta- and gamma-phase material following open-circuit stand periods in pressurized hydrogen.

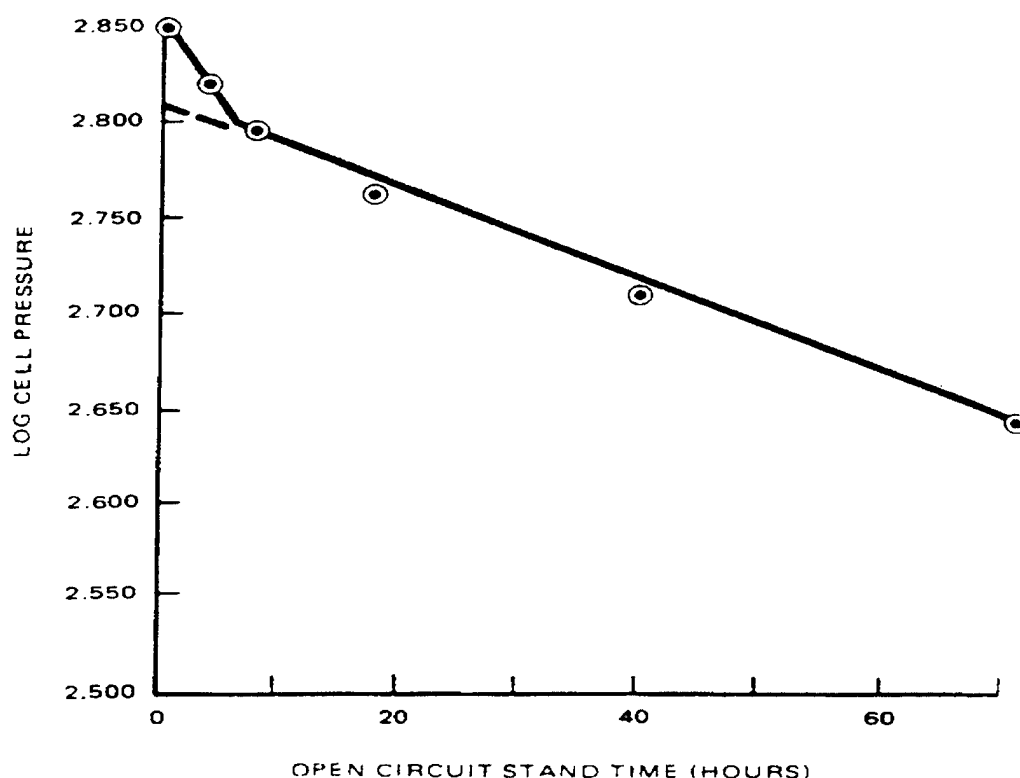


Figure 9. Loss of hydrogen pressure during open-circuit stand (from Ref. 5).



The cell was configured in the form of an electrode stack that was placed in a pressurized container, as depicted in Figure 10. The electrode stack was first charged using the same sequence as in the earlier experiments. Once it reached the EOC voltage, the electrode was placed on open circuit for an hour and then discharged against a nickel counter electrode. The potential of the nickel electrode was measured against a Hg/HgO reference electrode. The discharge curve, Figure 11, contains both gamma-phase and beta-phase material. Following the next changeup, the pressurized container was filled with hydrogen to a pressure of 400 psi, and the charged nickel electrode was allowed to soak in the high-pressure hydrogen for different lengths of time in the open-circuit condition. Following this, the hydrogen was removed, and the sweep from open-circuit voltage to full discharge was started at the rate of  $2 \mu\text{V/s}$ .

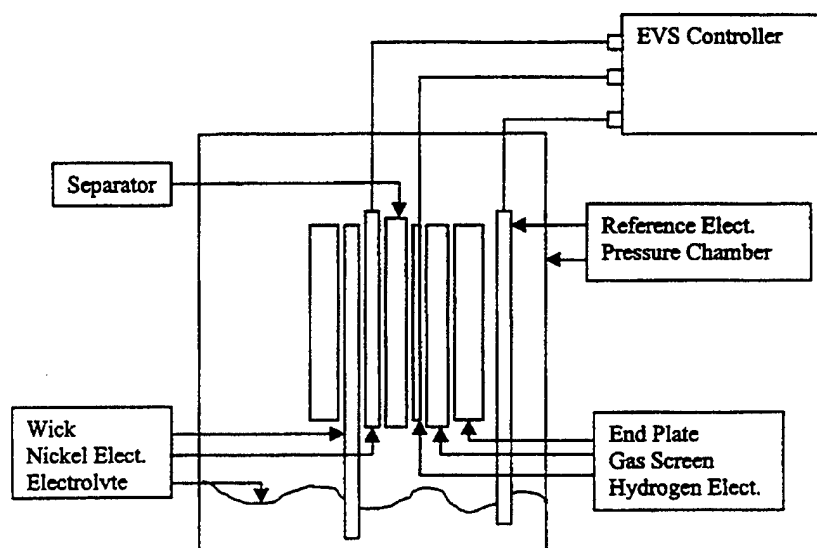


Figure 10. Cell configuration and test apparatus for hydrogen soak tests.

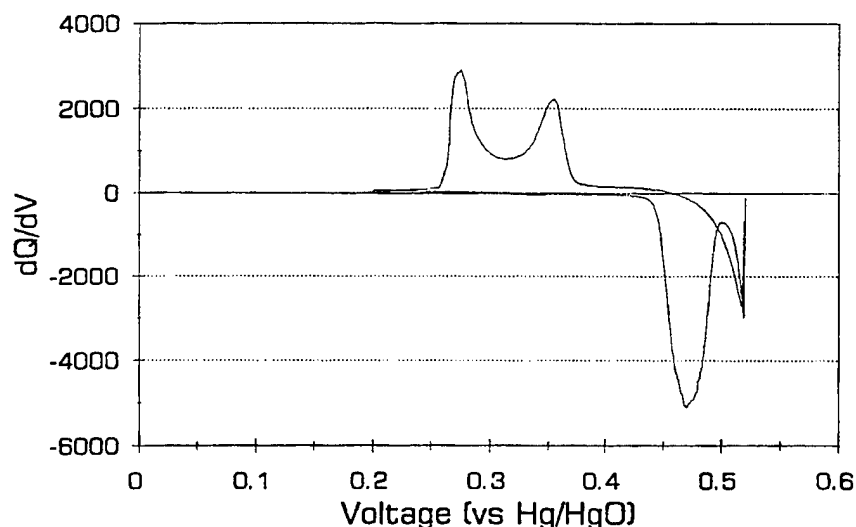


Figure 11. EVS spectra before exposure of charged nickel electrode to hydrogen gas.

The discharge scan of Figure 12, when compared with that in Figure 11, suggests that the first capacity to be lost upon exposure to hydrogen is some of the gamma material. This is in agreement with Ref. 7. These results are not entirely intuitive. Thermodynamic studies of the nickel electrode have determined that during the charge process, the gamma-phase material is thermodynamically more stable than the beta-phase material. Its half-cell voltage is about 40 mV less positive than the beta-phase reaction. Actual experience with the charging of nickel electrodes has demonstrated that the gamma-phase material is only obtained after the beta material has been formed as the electrode approaches full charge, where the competing oxygen evolution reaction occurs. Colder temperatures, higher concentrations of KOH, and higher levels of cobalt dopant in the nickel active material encourage the formation of gamma phase, but not at the expense of forming beta material first. The gamma phase does, however, spontaneously form at the expense of beta material whenever the beta material is not being cycled. This would be expected since the gamma phase is thermodynamically more stable.

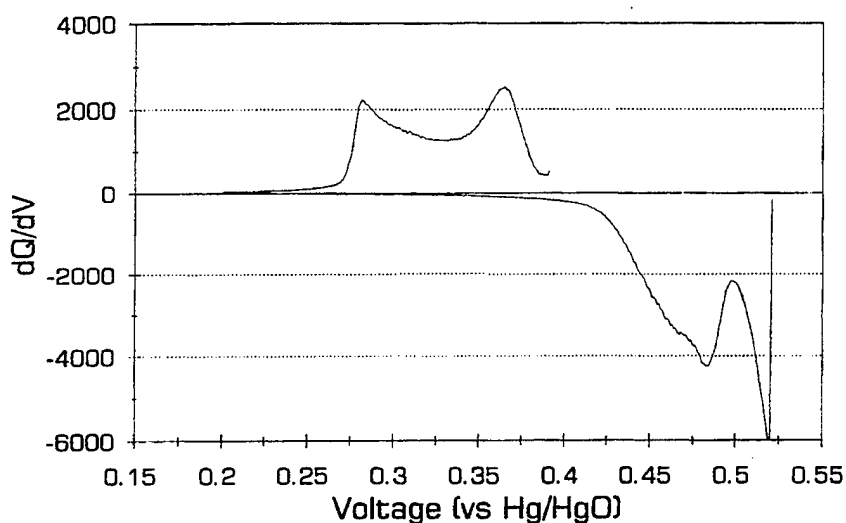


Figure 12. EVS spectra before exposure of charged nickel electrode to hydrogen gas.

## **5. Summary**

The EVS technique has proven to be a valuable electroanalytical technique for investigating the relative amounts of different phases present within the active material in sintered nickel electrodes. Electrodes that had been examined using other techniques were investigated in a series of tests in an attempt to identify signatures that would be associated with certain types of performance anomalies.

## References

1. Part 1, Chapter 1, *Handbook of Batteries and Fuel Cells*, Linden Editor in Chief, McGraw-Hill Book Company, 1984.
2. Kaufman, J. H., Chung, T. C., and Heeger, A. J., "Fundamental Electrochemical Studies of Polyacetylene," *J. Electrochem. Soc.*, Vol. 131, No. 12, pp 2847-2856, Dec. 1984.
3. Zimmerman, A. H., et. al., "Nickel Electrode Failure by Chemical Deactivation of Active Material," *Proceedings of the 1998 NASA Aerospace Battery Workshop*, Huntsville, AL, Oct 27-29, 1998.
4. Zimmerman, A. H., and Quinzio, M. V. "Causes for Cell Divergence in Nickel-Cadmium and Nickel-Hydrogen Cells," *Proceedings of the 14<sup>th</sup> Annual Battery Conference on Applications and Advances*, Long Beach, CA, Jan 12-15, 1999.
5. Suresh, M.S., and Subrahmanyam, A., "Effects of charged open-circuit stand in nickel-hydrogen cells," *Journal of Power Sources*, 50 (1994) 338-389.
6. Ritterman, P. F., and King, A. M., "The Open Circuit Stand Behavior of Intelsat VI Nickel-Hydrogen batteries and Its Relationship To Charge Rates and Temperature," *Proceedings of the 20<sup>th</sup> IECEC*, Vol.1, pp175-178, Miami Beach, FL, Aug 18-23, 1985.
7. Pralong, V., et. al., "Self-Discharge of the Nickel Electrode in Presence of Hydrogen II Electrochemical Approach," *J. Electrochemical Society*, Vol 146, (7), pp 2382-2386, (1999)

## TECHNOLOGY OPERATIONS

The Aerospace Corporation functions as an "architect-engineer" for national security programs, specializing in advanced military space systems. The Corporation's Technology Operations supports the effective and timely development and operation of national security systems through scientific research and the application of advanced technology. Vital to the success of the Corporation is the technical staff's wide-ranging expertise and its ability to stay abreast of new technological developments and program support issues associated with rapidly evolving space systems. Contributing capabilities are provided by these individual organizations:

**Electronics Technology Center:** Microelectronics, VLSI reliability, failure analysis, solid-state device physics, compound semiconductors, radiation effects, infrared and CCD detector devices, data storage and display technologies; lasers and electro-optics, solid state laser design, micro-optics, optical communications, and fiber optic sensors; atomic frequency standards, applied laser spectroscopy, laser chemistry, atmospheric propagation and beam control, LIDAR/LADAR remote sensing; solar cell and array testing and evaluation, battery electrochemistry, battery testing and evaluation.

**Mechanics and Materials Technology Center:** Evaluation and characterizations of new materials and processing techniques: metals, alloys, ceramics, polymers, thin films, and composites; development of advanced deposition processes; nondestructive evaluation, component failure analysis and reliability; structural mechanics, fracture mechanics, and stress corrosion; analysis and evaluation of materials at cryogenic and elevated temperatures; launch vehicle fluid mechanics, heat transfer and flight dynamics; aerothermodynamics; chemical and electric propulsion; environmental chemistry; combustion processes; space environment effects on materials, hardening and vulnerability assessment; contamination, thermal and structural control; lubrication and surface phenomena.

**Space and Environment Technology Center:** Magnetospheric, auroral and cosmic ray physics, wave-particle interactions, magnetospheric plasma waves; atmospheric and ionospheric physics, density and composition of the upper atmosphere, remote sensing using atmospheric radiation; solar physics, infrared astronomy, infrared signature analysis; infrared surveillance, imaging, remote sensing, and hyperspectral imaging; effects of solar activity, magnetic storms and nuclear explosions on the Earth's atmosphere, ionosphere and magnetosphere; effects of electromagnetic and particulate radiations on space systems; space instrumentation, design fabrication and test; environmental chemistry, trace detection; atmospheric chemical reactions, atmospheric optics, light scattering, state-specific chemical reactions and radiative signatures of missile plumes.

**Center for Microtechnology:** Microelectromechanical systems (MEMS) for space applications; assessment of microtechnology space applications; laser micromachining; laser-surface physical and chemical interactions; micropropulsion; micro- and nanosatellite mission analysis; intelligent microinstruments for monitoring space and launch system environments.

**Office of Spectral Applications:** Multispectral and hyperspectral sensor development; data analysis and algorithm development; applications of multispectral and hyperspectral imagery to defense, civil space, commercial, and environmental missions.